



Mapping aboveground biomass and carbon in Shanghai's urban forest using Landsat ETM + and inventory data



Guangrong Shen^{a,b,c,*}, Zijun Wang^{a,c}, Chunjiang Liu^{a,b,c}, Yujie Han^d

^a School of Agriculture and Biology and Research Centre for Low-Carbon Agriculture, Shanghai Jiao Tong University, 800 Dongchuan Rd., Shanghai 200240, China

^b Key Laboratory of Urban Agriculture, Ministry of Agriculture, China, Shanghai 200240, China

^c Shanghai Urban Forest Research Station, State Forestry Administration, China, 800 Dongchuan Rd., Shanghai 200240, China

^d Shanghai Forestry Station, 1053 Hutai Rd., Shanghai 200072, China

ARTICLE INFO

Handling Editor: Raffaele Laforteza

Keywords:

Remote sensing
Regression analysis
Residual
Spatial analysis
Urban forest

ABSTRACT

Quantifying the spatiotemporal distribution of **forest biomass carbon** (FBC) is vital for the management of urban forests in accordance with the rapid urbanization. This paper presents a method for quantifying and estimating the urban FBC in Shanghai, China, between 2005 and 2015, using data from 93 sampling forest plots and Landsat ETM + data. Our study included an analysis of the choice of predicted factors to estimate FBC and the method of carbon density estimation employed in the estimation. The results showed that combining regression analysis and spatial analysis to map forest carbon stocks at city level make available FBC estimates for the urban forests of Shanghai, China. Based on the proposal method, there was a decreasing trend of carbon density from downtown areas to outer suburban areas. About 92 % of the overall FBC storage in Shanghai distributed in the suburban areas whereas the urban areas shared a fraction amounting to only 8 % in 2015. From 2011–2015, the total urban forest carbon storage gradually increased by 32.3 %, whereas the average carbon density gradually decreased by 8.21 % in the urban areas. The associated values both increased continuously from 2005–2011, from 2005 to 2011, but the average carbon storage density decreased in the suburban districts. The total carbon stocks in the estimated forest biomass across Shanghai were about 1.5 Tg in 2005 and 2008, and 1.7 Tg in 2011 and 2015, while the associated average FBC density remained at about 17.5 t/ha from 2005 to 2015. This study provides important information required to manage the urban forest stand for optimal carbon sequestration.

1. Introduction

Forests biomass carbon (FBC) accounts for 77 % of the total carbon storage in global vegetation (Watson, 2000). Urban forest play a critical role in reducing atmospheric CO₂ and improving the urban environment in the process of photosynthesis and store excessive carbon as biomass (Mainknorn et al., 2011). In the context of addressing global warming, rapid urbanization and severe environmental problems, the international community has accepted forestry management as an effective method to mitigate increasing atmospheric CO₂ concentrations (Carretero et al., 2017; Zhang et al., 2013). Therefore, estimating and monitoring carbon sequestered in urban forests is essential for sustainable managers to leverage the mitigation potential of forests.

The morphological characteristics, functions, and structure of trees provide a wide range of ecosystem services and benefits that can alleviate the adverse effects of urbanization (Jian et al., 2019). There has

been much researches regarding the valuation, management, protection, and enhancement of these ecosystem services, particularly carbon storage (Vanessa, 2017). Several forest biomass and carbon models (such as i-Tree toolset and ENVI-met) using empirical and process-based techniques have been developed and implemented, that often apply biomass expansion/conversion factor or coefficient-based approaches, and integrate field inventory with remotely sensed data (Lu et al., 2014; Jian et al., 2019). Landsat Thematic Mapper (TM) imagery is easily accessed and is widely used since 1972 all over the world to estimate forest structural and functional attributes. Previous studies have developed techniques for the assessment of forest structures and functions using spectral vegetation indices (VIs) and spectral bands from ETM + remote sensing imagery (Cohen et al., 1995; Lu et al., 2014). Many researchers have achieved some degree of success in estimating forest biomass or carbon storage from TM data in natural areas worldwide (Viana et al., 2012; Ji et al., 2012; Phillips et al., 2016).

* Corresponding author at: School of Agriculture and Biology, Shanghai Jiao Tong University, 800 Dongchuan Rd., Shanghai 200240, China.
E-mail address: sgrong@sjtu.edu.cn (G. Shen).

However, the statistical relationships between FBC and VIs vary with the characteristics of ecosystem (Lu et al., 2014).

Compared with natural forests, urban forest usually is heterogeneous, fragmented, scattered, and surrounded by many impervious surfaces. Whether ETM + or ETM + imagery could still be used and which vegetation index extracted or spectral bands from TM (ETM +) imagery can be practically used for estimating urban FBC is still unknown. A few studies that have evaluated carbon storage in urban forests during the last few years were based on random sampling data (Carretero et al., 2017), National Forest Inventories data (Zhao, 2007) and LiDAR Strip Samples and Landsat Time-Series data (Ram et al., 2017). At the same time, the intensive dynamic of urban forest associated with urban expansion and urbanization, typically occurred in the urban-rural periphery (Portillo-Quintero et al., 2012). Excellent field-based methods exist for assessing urban forest distributions and volumes, but they are generally sample-driven and lack adequate detail for entire municipalities. The higher resolution remote sensing based carbon stock estimates sometimes are hardly reliable on both downtown and suburban areas (Phillips et al., 2016). In addition, these data are often more expensive and processing is time-consuming and laborious.

The integration of field plot aboveground biomass estimates with the 30-m Landsat ETM + data may provide a means, for mapping the spatial distribution of aboveground biomass of urban forest. However, the accuracy of forest aboveground biomass estimation using statistical techniques, that relate spectral variables and field plot aboveground biomass estimates, may be poor if an insufficient number of sample plots are used, or there is a weak linear relationship between spectral variables and aboveground biomass resulted may from mixed pixels. To be effective and make up for the deficiencies, it is crucial to develop a reliable method for accurately characterizing and quantifying the spatiotemporal pattern of urban forest at the appropriate scale, permitting mapping of aboveground biomass at a range of scales from downtown areas to outer suburban. In combination with Landsat TM (ETM +) remote sensing data, field inventor data and spatial analysis offers a solution to this mapping challenge.

The primary objective of this paper was to develop method based on Landsat TM (ETM +) remote sensing data and field inventor data to estimate and map FBC stock in Shanghai, China. We first developed the associated regression model between live aboveground biomass (AGB) derived from the permanent ground plot measurements of Shanghai Forestry Station, China (SFS) and VIs and/or spectral bands derived from Landsat data. Second, we computed the residual value of the regression model for each sampled site and upscaled them through interpolation. The AGB estimate model (at specified dates in time) at the city scale was constructed by integrating the regression model with the upscaled residuals. Lastly, the spatiotemporal distribution characteristics of FBC storage in Shanghai between 2005 and 2015 were analyzed in detail, and the distribution of changes, with respect to the accuracy associated with the process of modeling, was evaluated.

2. Materials and methods

2.1. Study area

Located on the eastern edge of the Yangtze River Delta between the latitudes 30°40'–31°53'N and longitudes 120°52'–122°12'E (Fig. 1), Shanghai in China is a typical international metropolis with an area of 6340 km² and a population density of 38 people/ha and forest coverage of 16.85 % in 2018. (<http://sh.sina.com.cn/news/m/2018-12-24/detail-ihqhqcir9662005.shtml>). According to the long-term functional orientation and administrative divisions, 977.1 km² in Shanghai is for the urban area (Huangpu, Xuhui, Changning, Putuo, Jing'an, Hongkou and Yangpu district) and 5,363.4 km² for the suburban area (Baoshan, Jinshan, Jiading, Minhang, Fengxian, Qingpu, Songjiang, Pudong and Chongming). The population density in Huangpu, Jing'an and Hongkou

district is over 300 people/ha while that is between 200–300 people/ha in Putuo and Yangpu district, and 50–100 people/ha for suburban districts (<http://baijiahao.baidu.com/s?id=1585560607763582557&wfr=spider&for=pc>). The urban forests and the green spaces of Shanghai have developed rapidly over the last two decades. The forest coverage increased from roughly 3.17 % in 1999, 12.58 % in 2009 to 14 % in 2014 (Viña et al., 2016), and to 16.85 % in 2018. (<http://sh.sina.com.cn/news/m/2018-12-24/detail-ihqhqcir9662005.shtml>). The prominent characteristics of the urban forest in Shanghai are wildly uneven among districts (Zhang, 2010). The native vegetation of Shanghai comprises of mixed evergreen and deciduous broad leaf forests. The largest fraction is *Cinnamomum camphora*, which account for 28 % of the total, while other stands are no more than 10 % of the total area of woodland such as *Metasequoia glyptostroboides* (5%) and *Demand Grandiflora Linn* (2%) (Wang et al., 2013; Xu, 2010; Zhang, 2010). A few small patches of natural secondary stands remain on the Jinshan Island and Sheshan Hill (Jun, 1997; Zhou, 1984). With the acceleration of industrialization and urbanization in recent years, the land-use type in Shanghai has constantly changed, especially in the suburban areas, where the agricultural land has been primary converted into plantations (Wang et al., 2011b). The Shanghai hold Expo took place in 2010 in an urban area, which occupied about 528 ha along the Huangpu River, and brought about significant local land use change. The forest cover in Shanghai has increased by 11 % during the past two decades owing to the implementation of fundamental forest projects (Li et al., 2013). Research has found that urban growth and the demand for land conversion has been driving urban-forested areas fragmentation and ecosystem changes (Wang et al., 2013; Xu, 2010). There are little data showing the contribution of changes in spatial-temporal patterns of FBC under rapid urbanization. Hence, reliable estimates and quantifying spatiotemporal pattern of urban forest biomass carbon at local to regional scales are required and investigated.

2.2. Field data

The field survey data used in this study was measured between June and October 2011 from 93 permanent plots of the regional forest inventory. These permanent plots were established by SFS according to the distribution of the plantations in terms of age and size (DBH) classes, and the corresponding soil properties. The permanent plots distributed across different districts and county in Shanghai. A sampling plot was required to be located in a relatively homogenous patch > 0.5 ha, Each of the 93 permanent sampling plots was defined as 28.3 m × 30 m (0.09 ha) to conform to a ETM + pixel size (Fig. 1).

The forest biomass refers to the AGB in this study, comprising the total biomass of root, stem, bark, branches and leaves. In the process of measurement and survey, "standard wood method of diameter rank" was used to collect the standard wood samples by taking 2 cm (or 5 cm for *Populus* cv. 'i-214') as the diameter grade through clipping from each tree type within a subplot. 1-2 plants were selected as standard trees in each diameter rank. Generally, 5-8 standard trees were selected for each tree species. The standard wood was excavated completely, and was sampled by roots, stems, branches and leaves, respectively, that then were taken to laborers and oven-dried until a constant dry biomass was achieved. A total of 110 standard trees were clipped in this experiment. Thus, with DBH as the relevant parameter to characterize the biomass, the biomass equations of the whole wood of 13 major tree species in Shanghai were established (Wang, 2012). The main data for the main tree species of Shanghai, including the mean diameter at breast height, mean tree height, and tree-age are shown in Table 1 (Wang, 2012). Hence, the above-ground dry biomass of each sampling plot were estimated using relevant tree biomass equations established above, and statistics and calculations for those trees biomass of direct AGB (kg/m²) measurements. The associated forest biomass carbon storage and carbon conversion rate were also measured (Wang, 2012).

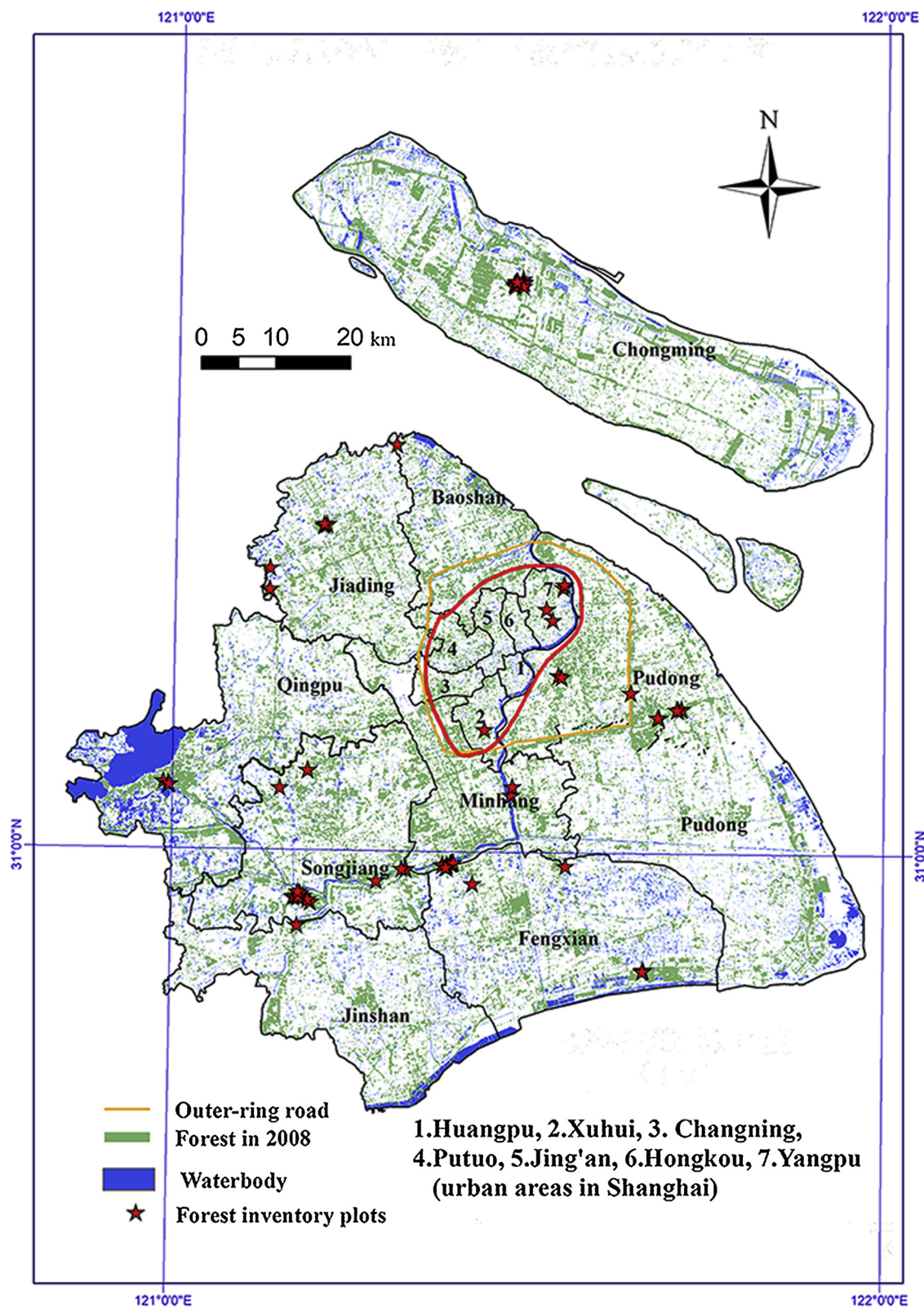


Fig. 1. Location of Shanghai and distribution map of forest inventory plots, and urban forest cover map for Shanghai in July of 2008.

2.3. Landsat data and processing

2.3.1. Landsat data

Two Landsat ETM+ scenes (path/row: 118/38 and 188/39, spatial resolution 30 m × 30 m) encompass the whole Shanghai area. Cloud-free images from the summer season (August 15th, 2005, July 6th,

2008, September 1st, 2011 and June 28th, 2015) were selected to capture stable phenological conditions and to avoid the seasonal changes. The Landsat ETM+ images were processed following the standard procedures, including atmospheric correction, relative radiometric normalization, and geometric correction, which were recommended for the detection of vegetation dynamics (Gómez et al.,

Table 1

Information on the different samples plots and the main tree species in Shanghai.

Forest type	Number of plots	Mean D (cm)	Mean H (m)	Tree-age (year)
<i>Cinnamomum camphora</i>	15	7.8–21	5.4–13.6	12–18
<i>Metasequoia glyptostroboides</i>	18	8.5–28.7	8.5–28.54	11–50
<i>Liquidambar formosana</i> Hance	2	9.2–12.8	7.9–10.3	12–30
<i>Taxodium ascendens</i>	4	9.4–17.3	8–14.6	12–30
<i>Sapindus</i>	3	8.3–8.8	6.7–7.7	12
<i>Koelreuteria integrifolia</i>	3	8.9–9.5	8.6–8.8	12
<i>Ligustrum lucidum</i>	3	10–10.9	7.7–8.6	12
<i>Ginkgo biloba</i>	6	6.5–13.8	2.6–6.4	12–25
<i>Elaeocarpus sylvestris</i>	7	10.7–13.6	6.6–8.4	11
<i>Magnolia Grandiflora</i> Linn	6	7.5–10.2	4.4–5.7	8–12
<i>Phyllostachys heterocycla</i>	5	8–9.3	11.2–11.8	2
<i>Populus euramericana</i>	3	14.9–17.7	11.6–14.5	12
Broad leaved mixed forest	18	6.7–17.4	4.1–17.2	10–15
total	93	5.7–28.7	2.6–28.4	2–50

Notes : D: diameter at breast height; H: height.

2014; Vicente-Serrano et al., 2008). These were performed for six bands of Landsat ETM+ (TM6 was excluded because of its coarse spatial resolution). Digital numbers (DNs) were converted to at-satellite reflectance values ρ , which is a unitless quantity denoting reflectance (Shen et al., 2015). This correction compensated for different sun angles at different acquisition dates. For each of the field plots, six reflectance values were extracted from the ETM+ spectral bands. The forest biomass estimation model was established based on the forest inventory and the ETM+ image from September 1st, 2011 because the field-observed data were acquired in the same period as the ETM+ image. The estimation model of forest biomass was applied in 2005, 2008 and 2015 after the radiometric correction between these multi temporal imageries.

2.3.2. Radiometric correction between two images

The radiometric correction methods based on pseudoinvariant features (PIFs), which show the potential for imagery-to-imagery radiometric normalization (Myeong et al., 2006), were employed to appropriately correct these multitemporal imagery for improved monitoring of changes over the study area. The image (of 2011) was used as the reference image to adjust the radiometric properties of all other images (from 2005, 2008, to 2015) to the same datum in solar geometry, sensor calibration, and environmental parameters as the reference image, and a linear relationship between the reference image (of 2011) and the subject images (2005, 2008, and 2015) was developed:

$$DN_{ref} = aDN_{sub} + b, \quad (1)$$

Where 'ref' is the reference image (the 2011 image), 'sub' is the subject image (the 2005, 2008, and 2015 images), a is the slope for the linear transformation, and b is the intercept for the linear transformation. The coefficients for images from 2005, 2008, and 2015 were found for Band7 and Band345 (Table 2).

2.3.3. Extraction of forest coverage information based on Landsat images

The spatial distribution maps of the urban forest for years 2005, 2008 (Fig. 1) and 2015 were produced through the supervised classification of color composite for the pre-processed ETM+ images using ERDAS 2018. In this paper, supervised classification(maximum likelihood classifier) was performed by means of training areas and supervised pixel-based image classification, and land cover classes were attributed based on field observations, Shanghai forest resource inventory information and real time Google earth imagery of the area. In

Table 2

The image normalization coefficients and the correction statistics for each subject image.

	2005		2008		2015	
	Band7	Band345	Band7	Band345	Band7	Band345
a	0.635	2.425	0.468	0.891	0.421	0.712
b	6.203	0.510	5.932	4.801	7.235	5.399
R^2	0.800	0.805	0.825	0.842	0.831	0.818

particular, the distribution information of *Cinnamomum camphora* that account for 28 % of the total is extracted based on Shanghai forest resource inventory information and remote sensing classification interpretation.

2.4. Methods

2.4.1. Relationships between AGB and satellite data

To develop a suitable estimation model, several spectral vegetation indices associated with the forest biomass and structure were extracted from the 2011 VIs map. These indices were the Normalized Difference Vegetation Index (NDVI), Ratio Vegetation Index (RVI), Difference Vegetation Index (DVI), Soil-Adjusted Vegetation Index (SAVI), and Modified Soil-Adjusted Vegetation Index (MSAVI) (Gómez et al., 2014). In addition, new images were synthesized through band combinations, such as the sum of ETM+ Band2, Band3, and Band4 (denoted Band234), and the sum of ETM+ Band3, Band4, and Band5 (denoted Band345), were used as alternative auxiliary parameters.

Correlation analysis between AGB at 93 sampling plots and satellite data of 2011 was performed using SPSS 19.1, to select the factors used in AGB estimation procedure. The potential variables used, such as ETM+ Band1, Band2, Band3, and others listed in Table 2, were chosen based on published literature. We found that ETM+ Band5, Band7, and Band234, Band345 have stronger relationships with the AGB than these vegetation indices, especially for forest sites with complex stand structures (Table 3).

2.4.2. Model development

The forest biomass variables were firstly subjected to stepwise regression against the auxiliary variables, Band5, Band7, and Band345, as selected above. Second, for each sampled plot, the residual value of the regression model was computed, and was then interpolated by Geostatistics to predict residual error in the unsampled sites. Finally, the forest biomass in the study area was estimated by combining the regression model based on remote sensing image data and the residual error spatial distribution map.

The procedure in detail as the following steps:

- (2) The optimal regression model was established by stepwise regression analysis between measured AGB and satellite data (Band5, Band7, Band345, etc.).

$$Z_0(x_i) = \sum_{j=1}^n \alpha_j V(x_j) + \alpha_0 \quad (2)$$

Where $Z_0(x_i)$ is an estimated biomass value of the regression model at sampled site i , $V(x_j)$ is the forest biomass decision variable ($p < 0.05$), α_j is the associated coefficient and n is the number of decision variables. In this study, the 62 observed samples data that were used to develop the AGB model were drawn from 93 plots through a stratified random sampling scheme, based on the stand age structure, tree composition, and distribution within Shanghai. The other 31 samples data of the 93 plots were used to validate the model performance. The resulting regression equation (Eq. (3)) was developed when the field forest biomass in 2011 was as the

Table 3

The correlation coefficient between the AGB and variables.

	Band1	Band2	Band3	Band4	Band5	Band7	NDVI	DVI	RVI	SAVI	MSAVI	Band234	Band345
AGB	-0.206	-0.184	-0.152	0.052	-0.638**	-0.585**	0.121	0.113	0.144	0.12	0.057	-0.248	-0.678**

Note : "****" denotes significant correlation at the 0.01bilateral level; "****" denotes significant correlation at the 0.05bilateral level.

dependent variable and Band7 and the new image Band345 as the independent variables that were determined through stepwise regression and considered the inter-correlation between the variables.

$$Y = 82.941 - 2.564 \times X_1 + 0.651 \times X_2, \quad (3)$$

Where Y is the urban forest biomass density (t/ha), and X_1 and X_2 are the values of Band7 and Band345, respectively. The R^2 and the $Adj-R^2$ with the 62 training samples were 0.66 and 0.64, respectively. The regression model indicated a good performance ($P < 0.05$) based on the F-test.

(3) For each sample site, the residual value was computed.

$$r(x_i) = Z(x_i) - Z_0(x_i) \quad (4)$$

Where $r(x_i)$ is the residual value and $Z(x_i)$ is the measured AGB value at sampled site i .

(4) A spatial analysis was performed using Geostatistics, where spatial interpolation is conducted to predict the residual error for the unsampled sites (Sales, 2007; Meer et al., 2012). The interpolated raster data [$r'(x)$] of the residual error in the study area [$r(x_i)$] were obtained in this way.

Based on Eq. (4), the residual error at sampled sites in this study was easily calculated, and the residual value distribution in Shanghai was produced through interpolation using ordinary kriging (OK, one kind of Geostatistics).

(5) The forest biomass estimated model for the entire study area was calculated as follows:

$$Z'(x) = Z_0(x) + r'(x) \quad (5)$$

Where $Z'(x)$ is estimated AGB value and $r'(x)$ is a residual value in space.

Thus, the AGB estimation model (denoted **SA regression model**) was obtained following Eq. (5), which combines the regression model of AGB (Eq. (3)) and spatial analyses of residual value.

To assess the SA regression model in the present study, the OK geostatistics method (denoted Geostatistical model) was employed to interpolate the measured AGB at sampling plots in Shanghai, and the regression model Eq. (3)(denoted Regression model) was used to estimate the AGB in Shanghai. The estimation accuracy of urban forest biomass in Shanghai by three models was analyzed and compared. The root mean square error (RMSE), the mean relative error (MRE), and the mean absolute error (MAE) were used to examine the model performance (Pereira et al., 2010), and quantify the difference between an estimator and a measured value.

3. Results

3.1. Spatial distribution of forest biomass

The urban forest biomass spatial distribution map of Shanghai for the year 2015 (Fig. 2a) was derived from the SA regression model.

The biomass density of urban forests in Shanghai was between 15 and 120 t/ha. Generally, the higher biomass density areas were concentrated mostly in urban areas, such as the northern Pudong New Area District and Huangpu District, which have high densities of plants, mature trees, and older forests. Suburban areas, such as the Qingpu and Jiading districts, had relatively low biomass densities, because the land use types in these areas consisted of industrial and agricultural land, and the forest is mostly young trees. The spatial distribution of forest biomass displayed a tendency towards high densities in northeastern

areas and low densities in the southwestern areas of Shanghai.

Cinnamomum camphora that distributes mostly in downtown areas, and accounts for 28 % of the total, its biomass density generally is between 20 and 110 t/ha. The areas with high biomass density (60–110 t/ha) are mostly concentrated in the central urban areas of Jing'an and Putuo district. The lower biomass density (30–50 t/ha) was distributed in Jinshan, Qingpu and other suburban counties.

The urban forest leaf biomass density in Shanghai is between 1 and 10 t/ha. The biomass density of forest leaves in central urban areas is generally higher than that in suburban areas and counties, with an average biomass density of 3.4 t /ha and 2.52 t /ha respectively.

To validate the amount and density distribution of forest biomass, the present study results were compared with those compiled from previously published literature in terms of accuracy of assessment. Taking Chongming County as an example, the amount and density of biomass were 0.8 Tg and 37.94 t/ha, respectively, in 2008 based on this study. The corresponding results were 0.982 Tg and 37.4 t/ha, respectively, based on the volume-to-biomass conversion model according to Wang et al. (Wang et al., 2011a). Furthermore, the amount of forest biomass in different districts and counties in 2008 (Fig. 2b) estimated in this study was generally in line with the forest area inventoried in the Forest Resources Planning and Design Survey (FRPDS) of 2009 (<http://cfdb.forestry.gov.cn:443>).

3.2. Temporal changes in FBC stock

Estimates of the urban FBC stock in Shanghai for years 2005, 2008, 2011, and 2015 were derived from the SA regression model and Eq. (1), by applying the 0.50 factor to convert dry biomass into carbon.

The distribution maps of the urban FBC density show a slight change in the spatial distribution pattern for the three periods of 2005–2008, 2008–2011, and 2011–2015 (Fig. 3a–c). The forest carbon density and carbon storage in Shanghai maintained a steady increase during the same periods. The mean forest carbon density across Shanghai increased from 17.41 t/ha in 2005 to 17.59 t/ha in 2008 and 18.6 t/ha in 2011, whereas it decreased to 17.59 t/ha in 2015. The corresponding forest carbon storage increased from 1.51 million tons (Tg) in 2005 to 1.57 Tg in 2008, 1.71 Tg in 2011, and 1.75 Tg in 2015. The carbon storage increased annually by 0.02 Tg from 2005 to 2008, by 0.04 Tg from 2008 to 2011, and by 0.015 Tg from 2011 to 2015. The change of the total biomass from 2005 to 2011 was also found to be in agreement with the FRPDS results for Shanghai in 2009 and other studies (Shi, 2009; Zhang, 2001).

As shown in Fig. 3d, the total amount of carbon stored in trees located in urban areas was minor compared to that of suburban areas such as the Qingpu and Jiading districts, in accordance with the proportions of the suburban(85 %) and urban areas (15 %) to the total Shanghai area, although trees in the suburban areas were younger. Accordingly, the carbon stored in forest leaves in suburban districts and central districts accounted for 94.16 % and 5.84 % respectively. The carbon stored in *Cinnamomum camphora* of dominant tree species in Shanghai accounted for 37.12 % of the total amount of carbon of urban forest in Shanghai.

The change in forest carbon densities in Shanghai was uneven for the period from 2005–2015. The area with carbon densities higher than 40 t/ha increased by 15.93 % from 2005 to 2011, whereas areas with carbon densities less than 10 t/ha decreased by 5.6 %. The intervening forest areas remained in the majority during the same period. The

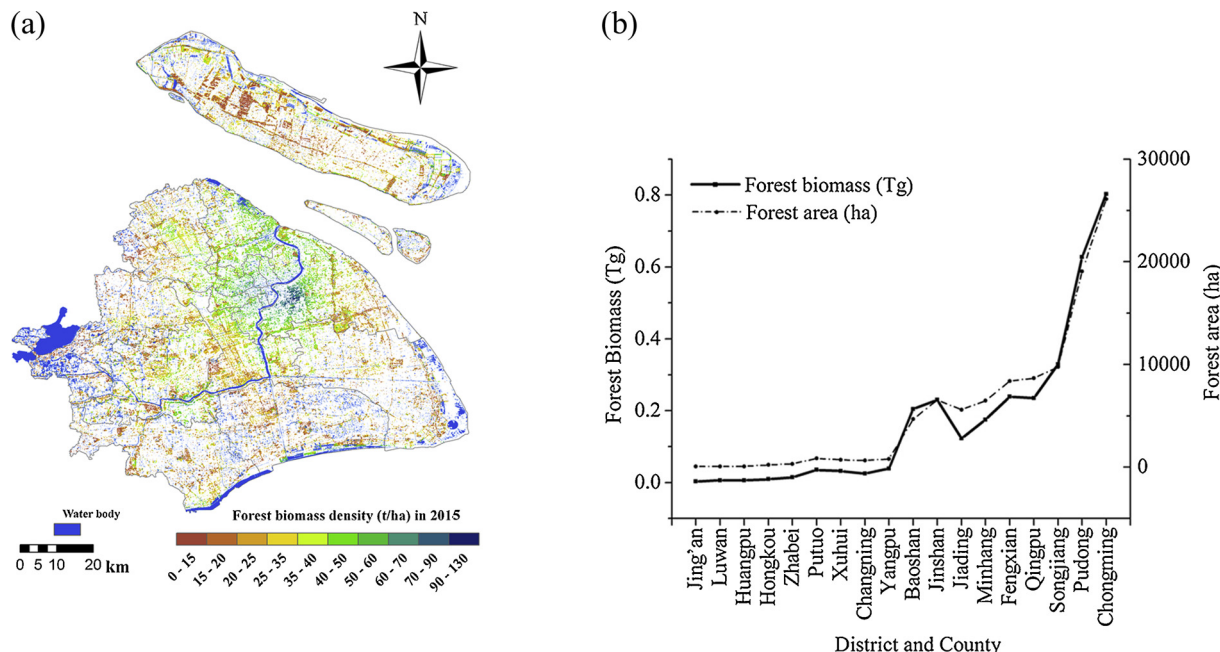


Fig. 2. a) Maps of the urban forest biomass density in Shanghai, China for the year 2015, and b) a chart of the forest biomass and the relative area in the year 2008.

dynamic change characteristics of urban forest carbon storage in Shanghai were closely associated with its rapid urbanization and some mega-events. With the construction of the World Expo 2010 ecological city, the forest biomass change in the urban and suburban areas of Shanghai showed a growing trend from 2008 to 2011, with increases of 10 % and 5 % in the forest area and the forest biomass, respectively. In the north Pudong New Area District, which occupied more than 70 % of the Expo planning area, the forest growth ratio of 2008–2011 was three times that of 2005–2008.

4. Discussion

The estimation accuracy of urban forest biomass in Shanghai from the SA regression model was analyzed, which was compared with that from Geostatistical model and Regression model (Eq. (3)) to assess the SA regression model in the present study.

The scatter plots of AGB at 31 sampling plots location against the predicted AGB by SA regression model, Regression model and the Geostatistical model were produced, respectively (Fig. 4). As illustrated in Fig. 4, R-squared of AGB predictions by SA regression model, Regression model and the Geostatistical model were 0.88, 0.33 and 0.94, respectively. The accuracy in terms of RMSE, MAE and MRE showed that the SA regression model, with an RMSE of 8.39, MAE of 6.86 and MRE of 24.22 %, displayed a high performance in comparison with the Regression model and the Geostatistical model (Table 4).

The advantage of the SA regression model was that the under- or over-estimated AGB from the Regression model was compensated for by introducing the spatial interpolated residual values of the estimated and measured biomass data. Meanwhile, the Geostatistical model depended alone on the sample data, and it was difficult to consider more to the fragmentation and heterogeneity of urban forests compared to that when using remote sensing data.

Our results showed that the SA regression model was an efficient way to retrieve the AGB, considering that the density of the urban forest biomass across Shanghai was uneven. For instance, in 2011, the density of Shanghai urban forest biomass (Fig. 5) ranged from 10–80 t/ha, and presented a spatially homogeneous distribution according to the Regression model. However, the associated residual errors ranged from –20 to 50 t/ha. The areas with higher residual errors were located in the northeast or the downtown area, whereas the areas with lower

residual errors were respectively in the northwest and the south, or the suburban areas. The predictions based on the Regression model may under- or over-estimate the urban forest AGB. Considering the example of a park located in Pudong New Area District, the measured biomass density was 121.51 t/ha, the corresponding value predicted from the Regression model was 60.96 t/ha, and the residual error was 60.55 t/ha. Similarly, in the Liantang sampling site in Qingpu District, the measured biomass density was 10.32 t/ha, the value obtained from the Regression model was 23.85 t/ha, and the residual error was –13.53 t/ha. This tendency most likely related to two factors: optical sensors have a limited sensitivity for reproducing the canopy structure of dense forests (such as in Pudong New Area District), which can lead to saturated estimates of biomass. There is also the confounding effect of understory vegetation in sparse and/or young forests, where forest biomass is generally low (such as in Liantang sampling site). The tendency of the Regression model to over-predict low biomass and under-predict high biomass conditions had also been discussed in previous studies (Blackard et al., 2008).

In a similar way, geostatistical analysis, which is dependent on the distribution and the number of sampling sites across the study area, may produce relatively monodispersed estimations for the urban forest biomass density (Sales, 2007; Meer et al., 2012). Comparison of the SA regression model with the Regression model and Geostatistical model over the area of Shanghai showed that the AGB estimates produced by the SA regression model derived with better accuracy. The RMSE, MRE, and MAE of the SA regression model (Table 4) improved by 11.4 %, 8.53 %, and 43.08 %, respectively, in comparison with the Regression model, and by 13.81 %, 9.67 %, and 45.78 %, respectively, in comparison with the Geostatistical model. It was then evident that the error factors RMSE, MRE, and MAE decreased faster for the SA regression model than for the Regression and the Geostatistical models (Table 4).

To summarize, as might be expected, the integrated modeling approach combining regression model and the spatial interpolation in the residual errors of the prediction showed obvious advantages for determining the spatial variability in forest biomass and structure, and the estimates of AGB dynamic between 2005–2015 were tested or validated by complementary regional studies (Shi, 2009; Zhang, 2001).

The average FBC density in the urban area of Shanghai (about 977.1 km²) estimated in the study was about 21.5 t/ha, which is within the average range of 1.92–32.68 t/ha estimated by Lin et al. (2007), and

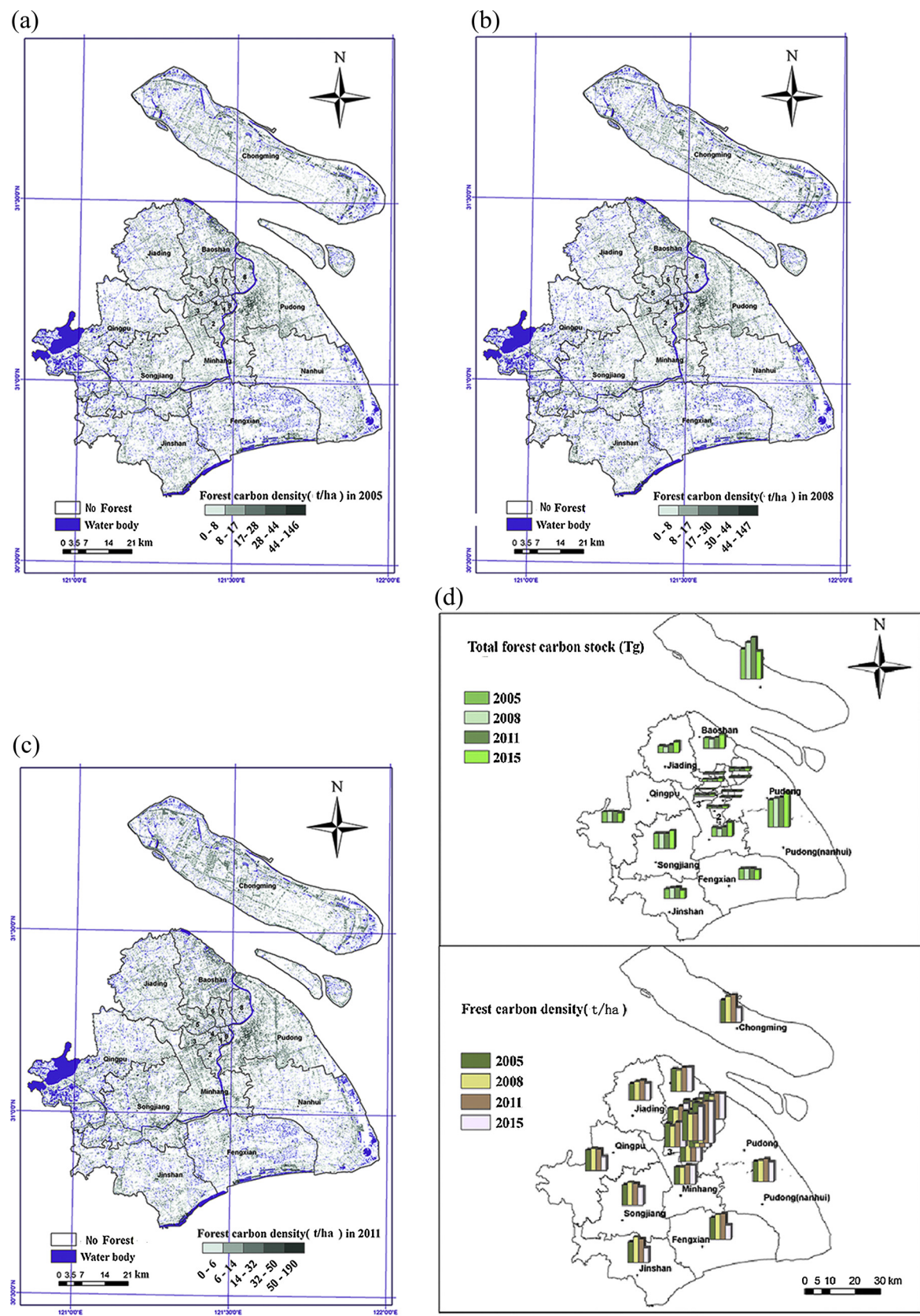


Fig. 3. Maps of the urban forest carbon density in Shanghai, China for the years 2005(a), 2008 (b), and 2011 (c), and the change in the total carbon amount and mean carbon density from 2005 to 2015 (d).

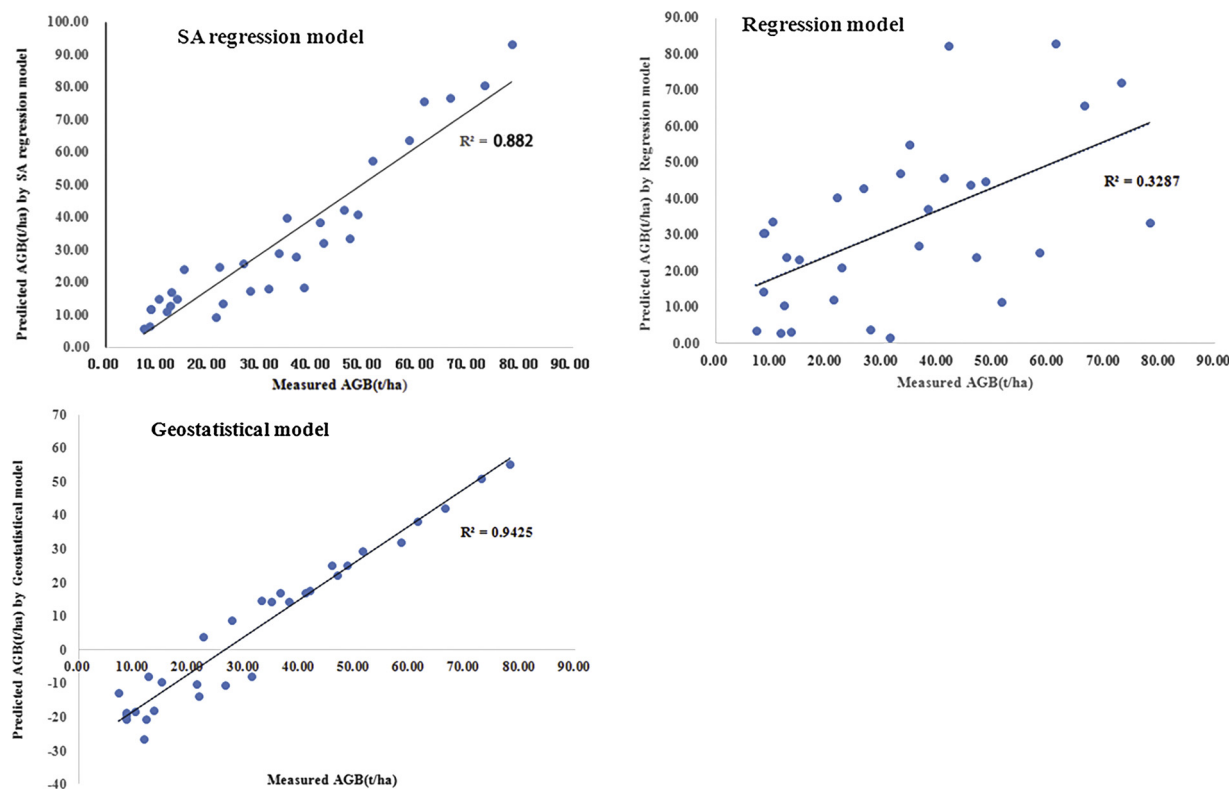


Fig. 4. Equivalence plot of aboveground biomass (AGB) predictions by the Regression model, Geostatistical model, and SA regression model.

Table 4

Accuracy comparison of the Regression model, Geostatistical model, and SA regression model, based on a sample population of 31 validation sites.

Model	RMSE	MAE	MRE
Regression model (Eq.(3))	19.83	15.39	67.3%
Geostatistical model	22.2	16.53	70 %
SA regression model	8.39	6.86	24.22 %

lower than the value of 47.8 t/ha estimated by Xu et al. (2010). The studies (Lin et al., 2008; Xu, 2010) reporting higher average AGB carbon estimates based on ground data and remotely sensed products. These studies focused on the downtown area of Shanghai; where there were higher densities of tree planting, the estimates were at the regional level, and the field-plots were in an area with relatively homogeneous forest distribution. On the contrary, the present study estimated the urban FBC in Shanghai at the city level, including both the urban and suburban areas, and hence, the field-plots were distributed across Shanghai as far as possible in order to provide a good representation of the environmental variation. These indicated that the scale, estimate approach, and associated data were very important when we evaluated the estimate results of urban FBC stocks.

Accordingly, there could still be some uncertainties in SA regression model and inaccuracies in model parameterization. The uncertainty reported in the final maps possibly originated from imprecision in the regression modeling, which combined a set of SFS plots representative of the present forest conditions, using spectral data captured by Landsat sensors. Forest spectral differences alone have been demonstrated to be inadequate for this purpose, as the heterogeneous and fragmented landscape in urban forest may result in a mixed pixel problem at various stages of the overall method, including the location of plots, field measures, allometric equations, and image processing (Campbell et al., 2012). In this case, high-resolution remote sensing image may be a more effective method to capture spectral data of sampling points. Furthermore, the spatial pattern of urban forest biomass and its change

could be analyzed at two scales such as urban and suburb area by using suitable remote sensing images (resolution, availability and cost performance, and image radiometric correction) when there were corresponding sampling plots. Therefore, the frequency and regularity of spectral measurements and sensitivity analyses can be critical, and should take into account while selecting accurate remote sensing and inventory-based forest parameters for improving AGB modeling.

5. Conclusion

The SA regression model was combining regression model with spatial analysis, based on a set of SFS plots representative of the present forest conditions and spectral data captured by Landsat sensors. The urban FBC were mapped in Shanghai over a period of 10 years (2005–2015) based on the proposal model.

More carbon is stored in suburban forests than in the downtown areas in Shanghai. The density and the amount of FBC in Shanghai maintained a steady increase from 2005 to 2015, while the pattern and dynamic change in the urban forest biomass were different between the urban and suburban areas, which was closely related to the urbanization and mega-events occurring in the metropolis.

From the results, we conclude that spectral and inventory data combined with the proposed SA regression model provide accurate biomass carbon estimates at a city scale, and monitoring the spatio-temporal patterns of heterogeneous urban forests is feasible when combining remote sensing with an upscaled prediction of the residual value. Our results also reinforce the need for more local sampling forest plots in order to improve the AGB estimation in urban forests by using remote sensing data, as well as additional sensitivity analyses and an assessment of understory reflectance (such as introducing VIs as factors) that might influence biomass modeling.

CRediT authorship contribution statement

Guangrong Shen: Conceptualization, Methodology, Software,

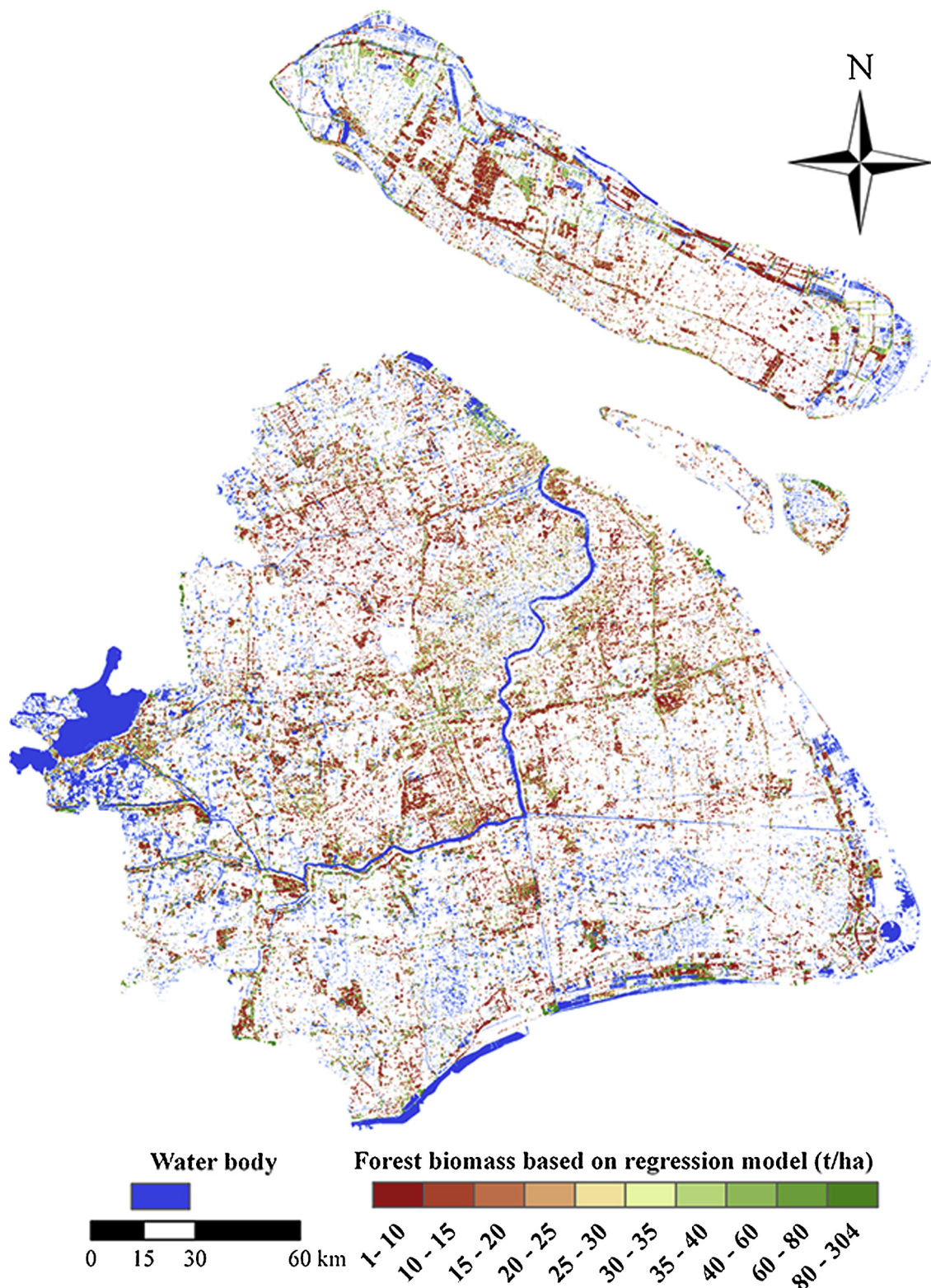


Fig. 5. Map of the spatial distribution of urban forest biomass based on the Regression model in Shanghai.

Writing - review & editing. **Zijun Wang:** Data curation, Writing - original draft. **Chunjiang Liu:** Supervision. **Yujie Han:** Visualization, Investigation.

Declaration of Competing Interest

The authors declare that they have no known competing financial

interests or personal relationships that could have appeared to influence the work reported in this paper

Acknowledgments

This research was supported by the National Key R&D Program of China (2017YFD0800204) and "Science and Technology Innovation

Action Plan of Shanghai, China" enterprise international science and technology cooperation project (17230732600).

Appendix A. Supplementary data

Supplementary material related to this article can be found, in the online version, at doi:<https://doi.org/10.1016/j.ufug.2020.126655>.

References

- Blackard, J.A., Finco, M.V., Helmer, E.H., Holden, G.R., Hoppus, M.L., Jacobs, D.M., et al., 2008. Mapping U.S. forest biomass using nationwide forest inventory data and moderate resolution information. *Remote Sens. Environ.* 112 (4), 1658–1677.
- Campbell, J.L., Kennedy, R.E., Cohen, W.B., Miller, R.F., 2012. Assessing the carbon consequences of western juniper (*Juniperus occidentalis*) encroachment across Oregon, USA. *Rangel. Ecol. Manag.* 65 (3), 223–231.
- Carretero, E.M., Moreno, Gabriela, Duplancic, Andrea, Abud, Adonis, Vento, Barbara, Jauregui, Jorge Alcalá, 2017. Urban forest of mendoza (Argentina): the role of *Morus alba* (Moraceae) in carbon storage. *Carbon Manag.* 8 (1), 1–8.
- Cohen, W.B., Spies, T.A., Fiorella, M., 1995. Estimating the age and structure of forests in a multi-ownership landscape of western Oregon, U.S.A. *Int. J. Remote Sens.* 16, 721–746.
- Gómez, C., White, J.C., Wulder, M.A., Alejandro, P., 2014. Historical forest biomass dynamics modelled with Landsat spectral trajectories. *ISPRS J. Photogramm. Remote. Sens.* 93 (7), 14–28.
- Ji, L., Wylie, B.K., Nossov, D.R., Peterson, B., Waldrop, M.P., Mcfarland, J.W., et al., 2012. Estimating aboveground biomass in interior alaska with landsat data and field measurements. *Int. J. Appl. Earth Obs. Geoinf.* 18, 451–461.
- Jian, L., Kroll, Charles N., Nowak, David J., Greenfield, Eric J., 2019. A review of urban forest modeling: Implications for management and future research. *Urban For. Urban Green.* 43, 126399.
- Jun, G., 1997. Study on the basic characteristics of natural vegetation, vegetation regionalization and protection of Shanghai. *Geogr. Res.* 16 (3), 82–88.
- Li, J., Zhu, F., Song, C., Wu, J., 2013. Spatiotemporal pattern of urbanization in Shanghai, China between 1989 and 2005. *Lands. Ecol.* 28 (8), 1545–1565.
- Lin, W., Wang, C., Zhao, M., et al., 2008. Estimation urban forests NPP based on forest inventory data and remote sensing. *Ecol. Environ.* 17 (2), 766–770.
- Lu, D., Chen, Q., Wang, G., Liu, L., Li, G., Moran, E., 2014. A survey of remote sensing-based aboveground biomass estimation methods in forest ecosystems. *Int. J. Digit. Earth* 9 (1), 63–105.
- Mainknorn, M., Moisen, G.G., Healey, S.P., Keeton, W.S., Freeman, E.A., Hostert, P., 2011. Evaluating the remote sensing and inventory-based estimation of biomass in the Western Carpathians. *Remote Sens.* 3 (7), 1427–1446.
- Meer, F.V.D., 2012. Remote-sensing image analysis and geostatistics. *Int. J. Remote Sens.* 33 (18), 5644–5676.
- Myeong, S., Nowak, D.J., Duggin, M.J., 2006. A temporal analysis of urban forest carbon storage using remote sensing. *Remote Sens. Environ.* 101 (2), 277–282.
- Pereira, P., Oliva, M., Baltrenaite, E., 2010. Modelling extreme precipitation in hazardous mountainous areas. Contribution to landscape planning and environmental management. *J. Environ. Eng. Landsc. Manag.* 18 (4), 329–342.
- Phillips, J., Duque, Á., Scott, C., Wayson, C., Galindo, G., Cabrera, E., Chave, J., Peña, M., Alvarez, E., Cárdenas, D., 2016. Live aboveground carbon stocks in natural forests of Colombia. *For. Ecol. Manage.* 374, 119–128.
- Portillo-Quintero, C.A., Sanchez, A.M., Valbuena, C.A., Gonzalez, Y.Y., Larreal, J.T., 2012. Forest cover and deforestation patterns in the Northern Andes (Lake Maracaibo Basin): a synoptic assessment using MODIS and Landsat imagery. *Appl. Geogr.* 35, 152–163.
- Ram, D., Matthew, R., Grant, D., Hans-Erik, A., Warren, C., Christopher, W., 2017. Evaluating site-specific and generic spatial models of aboveground forest biomass based on Landsat time-series and LiDAR strip samples in the Eastern USA. *Remote Sens.* 9 (6), 598. <https://doi.org/10.3390/rs9060598>.
- Sales, M.H., Souza, C.M., Kyriakidis, P.C., Roberts, D.A., Vidal, E., 2007. Improving spatial distribution estimation of forest biomass with geostatistics: a case study for Rondônia, Brazil. *Ecol. Modell.* 205 (1-2), 221–230.
- Shen, G.R., Ibrahim, A.N., Wang, Z., Ma, C., Gong, J., 2015. Spatial-temporal land-use/land-cover dynamics and their impacts on surface temperature in Chongming Island of Shanghai, China. *Int. J. Remote Sens.* 36 (15), 4037–4053.
- Shi, L.J., 2009. The Research on LUCC and Soil Organic Carbon Pool of Shanghai Based on RS and GIS. PhD diss.. East China Normal University.
- Viana, H., Aranha, J., Lopes, D., Cohen, W.B., 2012. Estimation of crown biomass of *Pinus pinaster* stands and shrubland above-ground biomass using forest inventory data, remotely sensed imagery and spatial prediction models. *Ecol. Modell.* 226 (1729), 22–35.
- Vicente-Serrano, S.M., Pérez-Cabello, F., Lasanta, T., 2008. Assessment of radiometric correction techniques in analyzing vegetation variability and change using time series of Landsat images. *Remote Sens. Environ.* 112 (10), 3916–3934.
- Viña, A., et al., 2016. Effects of conservation policy on China's forest recovery. *Sci. Adv.* 2.3 (2016), e1500965.
- Wang, Z., 2012. Studies on Carbon Stock in Shanghai Urban Forest. PhD diss.. Shanghai Jiao Tong University.
- Wang, Z., Cui, X., Yin, S., Shen, G.R., Han, Y.J., Liu, C.J., 2013. Characteristics of carbon storage in Shanghai's urban forest. *Sci. Bull.* 58 (10), 1130–1138.
- Wang, R.J., Zhao, M., Gao, J., 2011a. Carbon storage of main vegetation types of urban forest, Chongming Island of China. *Scientia Geographica Sinica* 31 (4), 490–494.
- Wang, Z., Han, Y., Kang, H., Sun, X., Zhu, Y., Che, S., Liu, C., 2011b. Differential effects of plantation forestry and agriculture on earthworm abundance and the heavy metals in suburban soils in Shanghai, eastern China. *Fresenius Environ. Bull.* 20 (11), 3006–3013.
- Watson, R.T., Noble, I.R., Bolin, B., Ravindranath, N.H., Verardo, D.J., Dokken, D.J., et al., 2000. Land use, land-use change, and forestry. A Special Report of the IPCC 4. pp. 375.
- Xu, F., Liu, W.H., Ren, W.L., Zhong, Q.C., Zhang, G.L., Wang, K.Y., 2010. Effects of community structure on carbon fixation of urban forests in Shanghai, China. *Chin. J. Ecol.* 3, 439–447.
- Zhang, K.X., 2010. Study on Community Ecology of Shanghai Green Belt and Ecological Benefits and Aesthetics Assessment of Its Plant Communities. PhD diss.. East China Normal University.
- Zhang, Q.F., Xia, L., 2001. Development dynamic, distribution pattern and scale characters of the parks system in Shanghai. *J. Chin. Landsc. Architect.* 1, 58–61.
- Zhang, H., Qi, Z.-f., Ye, X.-y., Cai, Y.-b., Ma, W.-c., Chen, M.-n., 2013. Analysis of land use/land cover change, population shift, and their effects on spatiotemporal patterns of urban heat islands in metropolitan Shanghai, China. *Appl. Geogr.* 44, 121–133.
- Zhao, M., Zhou, G.S., Gao, J., 2007. Estimating the value of urban forest fixation CO₂: a case study of Shanghai urban forest (in Chinese). *Ecol. Econ.* 8, 143–145.
- Zhou, X., 1984. The main Natural Vegetation Types of Shanghai and Their Distribution. PhD Diss. 8. East China Normal University, pp. 189–198 3.